

Deformation of Marchenko-Pastur distribution for the correlated time series

Masato Hisakado*

* *Nomura Holdings, Inc., Otemachi 2-2-2,
Chiyoda-ku, Tokyo 100-8130, Japan*

Takuya Kaneko†

†*International Christian University
Osawa 3-10-2, Mitaka,
Tokyo 181-8585, Japan*

(Dated: November 15, 2024)

Abstract

We study the eigenvalue of the Wishart matrix, which is created from a time series with temporal correlation. When there is no correlation, the eigenvalue distribution of the Wishart matrix is known as the Marchenko-Pastur distribution (MPD) in the double scaling limit. When there is temporal correlation, the eigenvalue distribution converges to the deformed MPD which has a longer tail and higher peak than the MPD. Here we discuss the moments of distribution and convergence to the deformed MPD for the Gaussian process with a temporal correlation. We show that the second moment increases as the temporal correlation increases. When the temporal correlation is the power decay, we observe a phenomenon such as a phase transition. When $\gamma > 1/2$ which is the power index of the temporal correlation, the second moment of the distribution is finite and the largest eigenvalue is finite. On the other hand, when $\gamma \leq 1/2$, the second moment is infinite and the largest eigenvalue is infinite. Using finite scaling analysis, we estimate the critical exponent of the phase transition.

I. INTRODUCTION

Random matrix theory (RMT) is a hot topic in several fields of physics and mathematics [1]. It has several applied fields, such as nuclear physics, machine learning, finance, and multiple-input multiple-output (MIMO) for wireless communication [2–7]. Separating the noise from the signal is one of the applications of RMT in finance [6, 8, 9]. For MIMO the transmission characteristic is ruled by the eigenvalues of the Wishart matrix. In fact, the channel capacity is calculated by the distribution of its eigenvalues.

In this article, we study a time series of financial data. We created the Wishart matrix [10, 11] using these data. When there is no correlation in the time series of the data, the distribution of the eigenvalues of the Wishart matrix converges to the Marchenko-Pastur distribution (MPD) [12] because of Brownian motion. In the MPD case there is an assumption that the independent random variables. We now discuss the convergence of the distribution of the eigenvalues of the Wishart matrix when there is temporal correlation. Here, we discuss the exponential and power decay cases. In MIMO studies, the correlations of the random matrix are important because we can improve the channel capacity in correlated fading environments using large eigenvalues [13–16]. The correlation represents the distance between the array antennas. In [16] for the exponential decay case, it was conjectured that the distance between the largest and the smallest eigenvalues of the Wishart matrix increases as the correlation increases using numerical simulations. We show this conjecture in this article.

In the time series of financial data, temporal correlations are important. We can observe temporal correlations in several time series. The exponential decay corresponds to a short memory, and the power decay corresponds to intermediate and long memories [17]. Power decays are sometimes observed in financial time series as fractional Brownian motion (fBm) which includes both long and short memories [18–21]. In this study, we use the fBm as the power decay case for the numerical simulations.

In [22], we calculated the eigenvalue distribution of the Wishart matrix and compared the moments with the MPD for 25 financial time series, which includes Crypt currencies, foreign exchange, commodities, government bonds, and stock indexes. Note that in the application of the random matrix to finance, the time series of the portfolio is usually used. In this case, the Wishart matrix is the correlation matrix of the portfolio. The eigenvalue

distribution of the Wishart matrix does not fit the MPD well because of the true correlation in the markets. In [5] and [6] how to separate true correlation and noise using random matrix theory was introduced. Here, we use the time series of one product. Therefore, the eigenvalue distribution of the Wishart matrix fits the MPD. In this case, the Wishart matrix is the correlation matrix for different time series. We show some examples that are shown in [22] in Table I and their properties are detailed in Table VII. We can confirm that the moments for the time series, SOY beans, VIX, and NKY225 fit well with the MPD. On the other hand, USD/CAD, EUR/CHF, and USD/CNH do not fit well. One of the reasons for fitness for MPD is the temporal correlations. In fact, the times series of USD/CAD, EUR/CHF, and USD/CNH have higher temporal correlations for the shortest time lag, and they are 0.2 or more in absolute value as shown in Table II. We believe that the process with temporal correlations is not adopted by MPD. What is the distribution instead of the MPD for these time series with temporal correlations? This problem has been discussed in [7, 23, 24] using the method of free probability theory and numerical simulations. In particular, in [23] the case of fBm was discussed. In [25–30] the perturbation of the Wishart matrices was discussed using correlations. A phase transition is observed in the model. In the small correlation, the eigenvalue spectrum is the same as MPD. We show the moments of this model in Appendix E. When the perturbation exceeds the threshold, we observe the emergence of a separated largest eigenvalue. The distribution is the same as MPD. Hence, the correlation of the perturbation model is smaller than our temporal correlation, as discussed below.

In this study, we study the effects of temporal correlations of random variables. The temporal correlation is the exponential decay and power decay. When there are temporal correlations, the eigenvalues converge to the deformed MPD. We show that the mean of the deformed MPD does not depend on the correlation and that the second moment increases as the temporal correlation increases. Hence, as the correlation increases, the distribution has a fatter tail and a higher peak. In the power decay case, we observe a phenomenon such as a phase transition. There are finite second moment and infinite second moment phases. When $\gamma > 1/2$ which is the power index of the temporal correlation, the second moment of the distribution and the largest eigenvalue are finite. On the other hand, when $\gamma \leq 1/2$, the second moment and the largest eigenvalue are infinite. In fact, phenomena such as phase transition depend on temporal correlation [31, 32]. A non-equilibrium phase transition with

TABLE I. Moments for the distribution of eigenvalues of the financial time series correlation matrix and the MPD. μ_i is the i -th moment of the MPD and the correlation matrix [22]. The standard deviations are shown in parentheses.

No.	Data	μ_2	μ_3	μ_4	μ_5	μ_6
	MPD	1.333	2.111	3.704	6.938	13.597
1	USD/CAD	1.419 (0.008)	2.448 (0.028)	4.716 (0.082)	9.732 (0.218)	21.038 (0.568)
2	EUR/CHF	1.430 (0.003)	2.494 (0.016)	4.856 (0.055)	10.113 (0.164)	22.032 (0.456)
3	EUR/GBP	1.402 (0.003)	2.385 (0.015)	4.533 (0.055)	9.237 (0.180)	19.738 (0.562)
4	SOY	1.333 (0.003)	2.111 (0.013)	3.703 (0.041)	6.933 (0.122)	13.569 (0.344)
5	VIX	1.336 (0.007)	2.117 (0.027)	3.713 (0.085)	6.960 (0.254)	13.669 (0.736)
6	NKY 225	1.324 (0.049)	2.081 (0.020)	3.637 (0.064)	6.819 (0.186)	13.433 (0.512)

TABLE II. Temporal correlation of the shortest time lag in the financial time series

No.	1	2	3	4	5	6
Data	USD/CAD	EUR/CHF	EUR/GBP	SOY	VIX	NKY 225
Corr	-0.35	-0.33	-0.32	-0.03	-0.03	-0.08

an order parameter occurs when the temporal correlation decays according to the power law [31]. In the case of [32] when the power index is less than one, the estimator converges slowly. They are in the non-equilibrium process and the transition point is $\gamma_c = 1$.

The remainder of this paper is organized as follows. In Section II, we introduce the time series and the creation of the Wishart matrix. In Section III, we discuss the distribution of the deformed MPD. In Section IV, numerical simulations are performed to confirm the deformed MPD. In section V, we study the phase transition of the deformed MPD. Finally, the conclusions are presented in Section VI.

II. TEMPORAL CORRELATION OF TIME SERIES AND RANDOM MATRIX

In this section we introduce the Wishart matrix of the time series with correlation. We consider the time series of a stochastic process, A_t , to be the variables at time t . In the case of financial data, we use the historical data of the return r_t as A_t . The return is defined using the market price, p_t as

$$r_t = \ln p_t - \ln p_{t-1}.$$

Here we set the normalization,

$$E(A_t) = 0,$$

and

$$V(A_t) = 1.$$

To introduce the temporal correlation, let $\{A_t, 1 \leq t \leq T\}$ be the time series of the stochastic variables of the correlated normal distribution with the following $T \times T$ correlation matrix,

$$D_{T-1} = \begin{pmatrix} 1 & d_1 & \cdots & d_{T-1} \\ d_1 & 1 & \ddots & \vdots \\ \vdots & \ddots & 1 & d_1 \\ d_{T-1} & \cdots & d_1 & 1 \end{pmatrix}, \quad (1)$$

which is a parameter for the time series. Here the temporal correlation function, d_t , is defined as the correlation between A_s and A_{s+t} such that

$$d_t = \text{Cov}(A_s, A_{s+t}), \quad (2)$$

in any s . This shows how the previous returns affect this return. In this article we consider the exponential decay and power decay cases. Note that we use the normalization of A_t . Here we fold the time series A_t , N times, where $T = N \times L$,

$$A = (\mathbf{A}_1, \mathbf{A}_{1+L}, \cdots, \mathbf{A}_{1+(N-1)L}), \quad (3)$$

where $\mathbf{A}_\mu = (A_\mu, \cdots, A_{\mu+L-1})^T$, $\mu = 1, 1+L, \cdots, 1+(N-1)L$, is the size L vector and \mathbf{X}^T is the transpose of the vector \mathbf{X} . \mathbf{A}_μ is the time series from μ to $\mu+L-1$. A is the $L \times N$ matrix. In the application of the random matrix to the finance, \mathbf{A}_μ usually corresponds to the different product time series [5, 6], but here we use one product.

In the matrix form we can rewrite the $L \times N$ matrix form

$$A = \begin{pmatrix} A_1 & A_{L+1} & \cdots & A_{(N-1)L+1} \\ A_2 & A_{L+2} & \cdots & \vdots \\ \vdots & \ddots & \ddots & A_{NL-1} \\ A_L & \cdots & A_{(N-1)L} & A_{NL} \end{pmatrix}. \quad (4)$$

Note that here we consider the case $L \gg 1$. Hence,

$$d_i = \text{Cov}(A_s, A_{i+s}) = 0,$$

$i \geq L$.

We consider the relation between the non correlated random time series and the correlated ones. Here we consider the $L \times N$ matrix A_0 for non correlated time series. The elements of A_0 are i.i.d. Here we introduce the $L \times L$ matrix Π . The relation between the matrix A and A_0 is

$$A = \sqrt{\Pi}A_0, \quad (5)$$

where

$$\Pi = \sqrt{\Pi}\sqrt{\Pi}^T = D_{L-1}. \quad (6)$$

$\sqrt{\Pi}$ is the lower triangle matrix which is created by Cholesky decomposition [25]. We show Eq.(5) and Eq.(6) in Appendix F in detail.

Next we consider the Wishart matrix of A . The Wishart matrix is the correlation matrix $C_{i,j}$ which is a symmetric matrix and the diagonal elements are 1,

$$C_{i,j} = \frac{1}{L} \sum_{k=1}^L A_{(i-1)L+k} A_{(j-1)L+k}, \quad (7)$$

where $1 \leq i, j \leq N$. Note that $C_{i,j} = C_{j,i}$, when $i \neq j$ and $C_{i,i} = 1$ because of the normalization. In the matrix form,

$$C = \frac{1}{L} A^T A = \frac{1}{L} (\sqrt{\Pi}A_0)^T \sqrt{\Pi}A_0, \quad (8)$$

where A^T is the transposed matrix of A and C is $N \times N$ matrix.

When there is no correlation case, $A = A_0$, the distribution of the eigenvalues of C converges to the Marchenko-Pastur distribution (MPS) [12] in the double scaling limit, $N, L \rightarrow \infty$ with $L/N = Q$. When $A \neq A_0$, the distribution of the eigenvalues of C converges in the double scaling limit, $N, L \rightarrow \infty$ with $L/N = Q$ to a distribution, the deformed MPD which is different from MPD.

III. CONVERGENCE TO DEFORMED MARCHENKO-PASTUR DISTRIBUTION

In this section we calculate the moments of the deformed MPD. These are new results of this paper and we show the conjecture of [16]. Here we consider the case $d_i \rightarrow 0$, when $i \gg 1$. This means that the temporal correlation decays as time goes by. We calculate the k -th moment of the eigenvalue distribution of the Wishart matrix, C ,

$$\mu_k = \frac{1}{L^k N} \langle \sum_{j=1}^N (x_j)^k \rangle = \frac{1}{N} \langle \text{Tr}(C^k) \rangle, \quad (9)$$

where x_j is the eigenvalues of C and $\langle \rangle$ means the ensemble average. The moment of the MPD is in Appendix A.

i. First moment

$$\mu_1 = \frac{1}{LN} \sum_{\nu=1}^L \sum_{m=1}^N \langle (A_{\nu m})^2 \rangle = 1, \quad (10)$$

in the limit of $N, L \rightarrow \infty$ with $L/N = Q$. Note that it does not depend on the type of correlation decay. The mean of the distribution that does not depend on the temporal correlation is 1.

ii. Second moment

$$\begin{aligned} \mu_2 &= \frac{1}{L^2 N} \sum_{\nu_1=1}^L \sum_{\nu_2=1}^L \sum_{m_1=1}^N \sum_{m_2=1}^N \langle A_{m_1 \nu_1}^T A_{\nu_1 m_2} A_{m_2 \nu_2}^T A_{\nu_2 m_1} \rangle \\ &= \frac{1}{L^2 N} \sum_{\nu_1=1}^L \sum_{\nu_2=1}^L \sum_{m_1=1}^N \sum_{m_2=1}^N \langle A_{\nu_1 m_1} A_{\nu_1 m_2} A_{\nu_2 m_2} A_{\nu_2 m_1} \rangle = 1 + \frac{1}{Q} + \frac{2}{Q} \sum_{i=1}^2 d_i^2, \end{aligned} \quad (11)$$

in the limit of $N, L \rightarrow \infty$ with $L/N = Q$. Here we assume $d_L \sim 0$ in this limit, because

$$\langle A_j, A_{j+L} \rangle = 0,$$

in the limit $L \rightarrow \infty$. The first and second terms of Eq.(11) are for the MPD. The third term is for the temporal correlation. It is the sum of the cases, $m_1 \neq m_2$ and $\nu_1 \neq \nu_2$. It is

$$\frac{1}{L^2 N} \sum_{\nu_1 \neq \nu_2} \sum_{m_1 \neq m_2} \langle A_{\nu_1 m_1} A_{\nu_1 m_2} A_{\nu_2 m_2} A_{\nu_2 m_1} \rangle = \frac{N(N-1)}{L^2 N} \sum_{|\nu_1 - \nu_2|} \langle A_{\nu_1 m_1} A_{\nu_2 m_1} \rangle^2$$

$$= \frac{2N(N-1)L}{L^2N} \sum_i d_i^2 = \frac{2}{Q} \sum_{i=1} d_i^2. \quad (12)$$

The second moment of Eq.(11) increases as the temporal correlation increases. Then the deformed MPD has a longer tail than the MPD. When the second moment is finite, there is the finite largest eigenvalue. On the other hand, the second moment is infinite, and the largest eigenvalue is infinite. We discuss phenomena such as phase transition in the subsection for the power decay case.

A. Exponential Decay case

We consider the exponential decay case, $d_i = \text{Cov}(A_s, A_{i+s}) = r^i, 0 \leq r \leq 1$ and calculate the moments. r is the effect at t from the past at $t-1$. It is a used temporal correlation for financial time series. Here we set

$$A_{t+1} = rA_t + \sqrt{1-r^2}\xi_t, \quad (13)$$

where ξ_t is i.i.d. and we obtain the exponential decay to create a time series with exponential decay, $\langle A_{t+1}, A_t \rangle = r$. $\sqrt{\Pi}$ is

$$\sqrt{\Pi} = \begin{pmatrix} 1 & 0 & \dots & 0 \\ r & \sqrt{1-r^2} & 0 & \vdots \\ r^2 & r\sqrt{1-r^2} & \sqrt{1-r^2} & 0 \\ \dots & \dots & \dots & \dots \\ r^{L-1} & r^{L-2}\sqrt{1-r^2} & \dots & \sqrt{1-r^2} \end{pmatrix}, \quad (14)$$

and

$$D_{L-1} = \sqrt{\Pi}\sqrt{\Pi}^T = \begin{pmatrix} 1 & r & \dots & r^{L-1} \\ r & 1 & \ddots & \vdots \\ \vdots & \ddots & 1 & r \\ r^{L-1} & \dots & r & 1 \end{pmatrix}. \quad (15)$$

i. Second moment

The second moment is

$$\mu_2 = \frac{1}{L^2N} \sum_{\nu_1=1}^L \sum_{\nu_2=1}^L \sum_{m_1=1}^N \sum_{m_2=1}^N \langle A_{m_1\nu_1}^T A_{\nu_1 m_2} A_{m_2\nu_2}^T A_{\nu_2 m_1} \rangle$$

$$= 1 + \frac{1}{Q} + \frac{2}{Q} \frac{r^2}{1-r^2}, \quad (16)$$

in the limit of $N, L \rightarrow \infty$ with $L/N = Q$. The first and second terms are for the MPD. The third term is for the deformation for the correlation.

ii. Third moment

The third moment is

$$\begin{aligned} \mu_3 &= \frac{1}{L^3 N} \sum_{\nu_1=1}^L \sum_{\nu_2=1}^L \sum_{\nu_3=1}^L \sum_{m_1=1}^N \sum_{m_2=1}^N \sum_{m_3=1}^N \langle (A_{m_1 \nu_1}^T A_{\mu_1 n_2} A_{m_2 \nu_2}^T A_{\nu_2 m_3} A_{m_3 \nu_3}^T A_{\nu_3 m_1}) \rangle \\ &= 1 + \frac{3}{Q} + \frac{1}{Q^2} + \frac{6}{Q^2} \frac{r^4}{(1-r^2)^2} + \frac{6}{Q^2} \frac{r^2}{1-r^2} + \frac{6}{Q} \frac{r^2}{1-r^2}, \end{aligned} \quad (17)$$

in the limit of $N, L \rightarrow \infty$ with $L/N = Q$. The first, second and third terms are of the MPD. The rest of the terms are for the deformation for the correlation. The fourth term is for the case, $\nu_i \neq \nu_j$ and $m_k \neq m_l$, where i, j, k, l are 1, 2, 3, respectively. The fifth term is for the case $m_i = m_j \neq m_k$. It is one pair of m_i that has same values. The sixth term is for the case $\nu_i = \nu_j \neq \nu_k$. It is one pair of ν_i which have the same values.

iii. Fourth moment

The fourth moment is

$$\begin{aligned} \mu_4 &= \frac{1}{L^4 N} \sum_{\nu_1, \nu_2, \nu_3, \nu_4=1}^L \sum_{m_1, m_2, m_3, m_4=1}^N \langle (A_{m_1 \nu_1}^T A_{\nu_1 m_2} A_{m_2 \nu_2}^T A_{\nu_2 m_3} A_{m_3 \nu_3}^T A_{\nu_3 m_4} A_{m_4 \nu_4}^T A_{\nu_4 m_1}) \rangle \\ &= 1 + \frac{6}{Q} + \frac{6}{Q^2} + \frac{1}{Q^3} \\ &\quad + \frac{24}{Q^3} \frac{r^6}{(1-r^2)^3} + \frac{24}{Q^3} \frac{r^4}{(1-r^2)} + \frac{24}{Q^3} \frac{r^4}{(1-r^2)^2} + \frac{24}{Q^3} \frac{r^2}{(1-r^2)} \\ &\quad + \frac{24}{Q^2} \frac{r^4}{(1-r^2)^2} + \frac{12}{Q^2} \frac{r^2}{(1-r^2)} + \frac{24}{Q} \frac{r^2}{(1-r^2)}, \end{aligned} \quad (18)$$

in the limit of $N, L \rightarrow \infty$ with $L/N = Q$. The first four terms are for the MPD. The rest of the terms are for the deformation for the correlation. The fifth term is for any ν_i and m_j which do not have the same values. The sixth and seventh terms are for one pair which have the same values in m_i . The eighth term is for two pairs which have the same values in m_i . The ninth term is for one pair which has the same values in ν_i . The tenth term is for

one pair which has the same values in ν_i and one pair which has same values in m_i . The eleventh term is for two pairs which have same values in ν_i .

B. Power decay case

In this section we consider the case of power decay, $d_i = \text{Cov}(A_s, A_{i+s}) = 1/(i+1)^\gamma$ where γ is the power index. The second moment converges to the finite, when $\gamma > 1/2$,

$$\begin{aligned}
\mu_2 &= \frac{1}{L^2 N} \sum_{\mu_1=1}^L \sum_{\mu_2=1}^L \sum_{m_1=1}^N \sum_{m_2=1}^N \langle (A_{m_1 \mu_1}^T A_{\mu_1 m_2} A_{m_2 \mu_2}^T A_{\mu_2 m_1}) \rangle \\
&= 1 + \frac{1}{Q} + \frac{2}{Q} \sum_{i=1}^{\infty} \frac{1}{(i+1)^{2\gamma}} \\
&< 1 + \frac{1}{Q} + \frac{2}{Q} \int_1^{\infty} \frac{1}{(x+1)^{2\gamma}} dx \\
&= 1 + \frac{1}{Q} + \frac{2^{2-2\gamma}}{(2\gamma-1)Q}, \tag{19}
\end{aligned}$$

in the limit of $N, L \rightarrow \infty$ with $L/N = Q$. On the other hands, $\gamma \leq 1/2$,

$$\begin{aligned}
\mu_2 &= 1 + \frac{1}{Q} + \frac{2}{Q} \sum_{i=1}^{\infty} \frac{1}{(i+1)^{2\gamma}} \\
&> 1 + \frac{1}{Q} + \frac{2}{Q} \int_2^{\infty} \frac{1}{(x+1)^{2\gamma}} dx \\
&\sim \lim_{x \rightarrow \infty} \frac{2}{(1-2\gamma)Q} x^{-2\gamma+1}. \tag{20}
\end{aligned}$$

The second moment becomes infinite and the transition point is $\gamma_c = 1/2$.

If $x_1 < \infty$ which is the largest eigenvalue and $\sum_i x_i/N \rightarrow 1$ in the limit $N \rightarrow \infty$, then $\sum_i x_i^2/N < \infty$. This means finite μ_2 . Conversely if $x_1 \rightarrow \infty$ and $\sum_i x_i/N \rightarrow 1$ in the limit $N \rightarrow \infty$, $\sum_i x_i^2/N \rightarrow \infty$. This means infinite μ_2 . Therefore, we can conclude finite μ_2 corresponds to finite x_1 and infinite μ_2 corresponds to infinite x_1 . Therefore, it is also a phenomenon like the phase transition between the finite x_1 and the infinite x_1 .

IV. NUMERICAL SIMULATIONS

In this section we confirm the conclusions of section III using numerical simulations.

A. Exponential Decay

i. Deformed MPD

First, we confirm the deformed MPD. We calculated 1000 times each r and created a histogram of the eigenvalues. The conclusions are shown in Fig. 1. We can confirm that the distributions have a fat tail and a high peak for large r and the mean of the distribution is constant. On the other hand, for small r , the distributions have almost the same shape as the MPD.

ii. Convergence of the moments

Next, we confirm the convergence of the distributions for the exponential decay case. In Fig.2 we show the convergence of the moments, μ_2 and μ_3 . The horizontal axis is r and the vertical axis represents the second and third moments. As the matrix size increases, the moments converge to the theoretical ones. In Appendix C, we present the conclusions of numerical simulations in detail.

B. Fractional Brownian motion

Next, we confirm the fractional Brownian motion (fBm) case which has power decay temporal correlations and fBm is observed in the financial time series. The relation of the indexes is

$$2 - 2H = \gamma, \tag{21}$$

where H is the Hurst index for fBm and γ is the power index. Hence, the transition point is, $H_c = 3/4$ which corresponds to $\gamma_c = 1/2$. We explain fBm in Appendix B.

i. Deformed MPD

First, we confirm the distributions of the deformed MPD for the fBm case. We calculated 100 times for each H and created a histogram of the eigenvalues. The conclusions are shown in Fig.3. We can confirm the difference from the MPD in smaller H and larger H . On the other hand for around $H = 0.5$, the distributions have almost the same shape as the MPD,

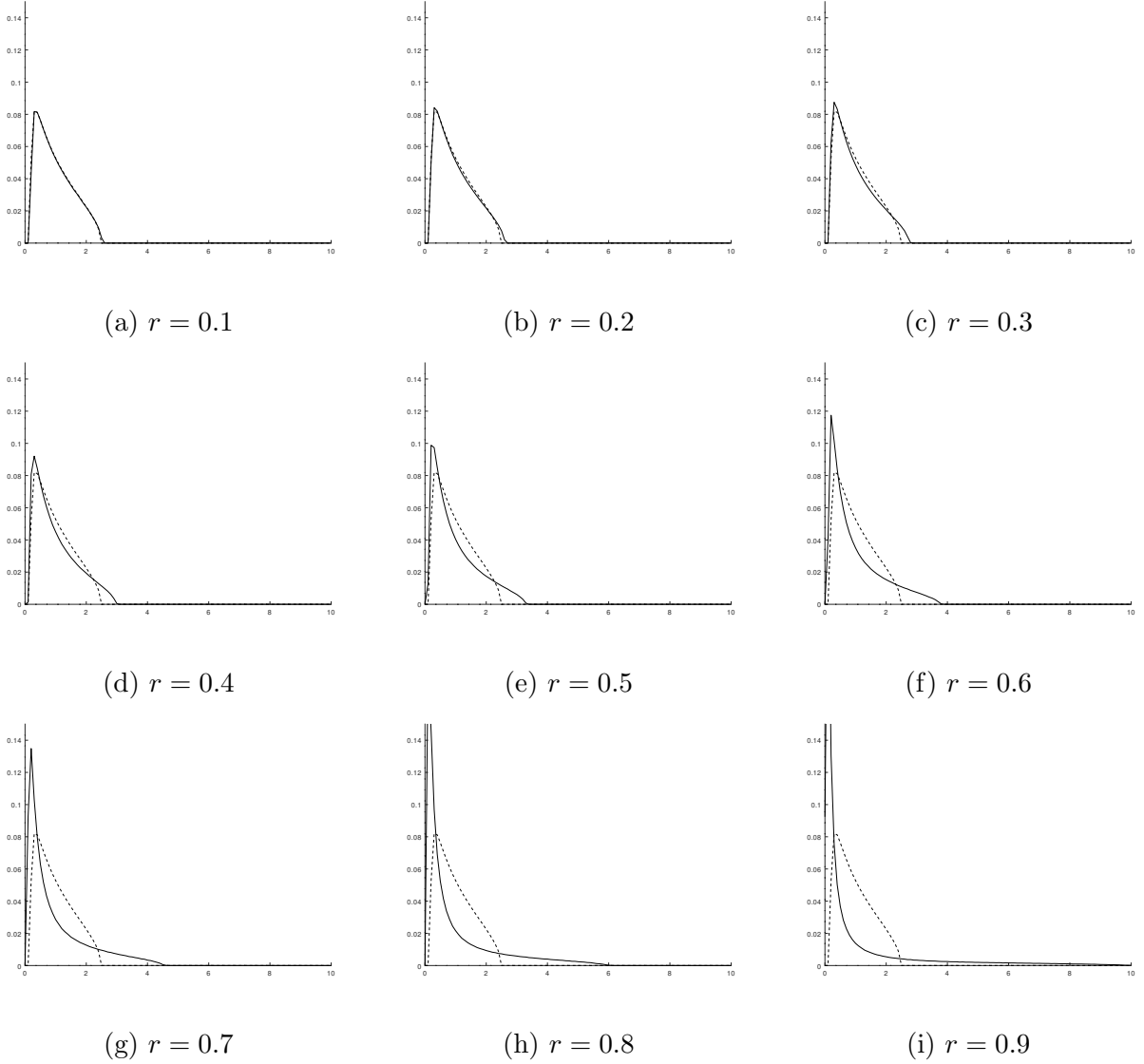


FIG. 1. Plots of histogram of the deformed MPD for $Q = 3$: (a) $r = 0.1$, (b) $r = 0.2$, (c) $r = 0.3$, (d) $r = 0.4$, (e) $r = 0.5$, (f) $r = 0.6$, (g) $r = 0.7$, (h) $r = 0.8$, (i) $r = 0.9$. The horizontal axis is the eigenvalue and the vertical axis is the frequency. The real line is the distribution with the correlation and the dotted line is the MPD. We can confirm the fat tail of the distribution for large r and the mean is constant.

because $H = 1/2$ is the Brownian motion. Above $H_c = 3/4$, there is a phase transition and we can observe large eigenvalues. In fact we can observe the peak at 10 in $H = 0.8$ and 0.9 in Fig.3 (h) and (i) which corresponds to the large eigenvalues above 10.

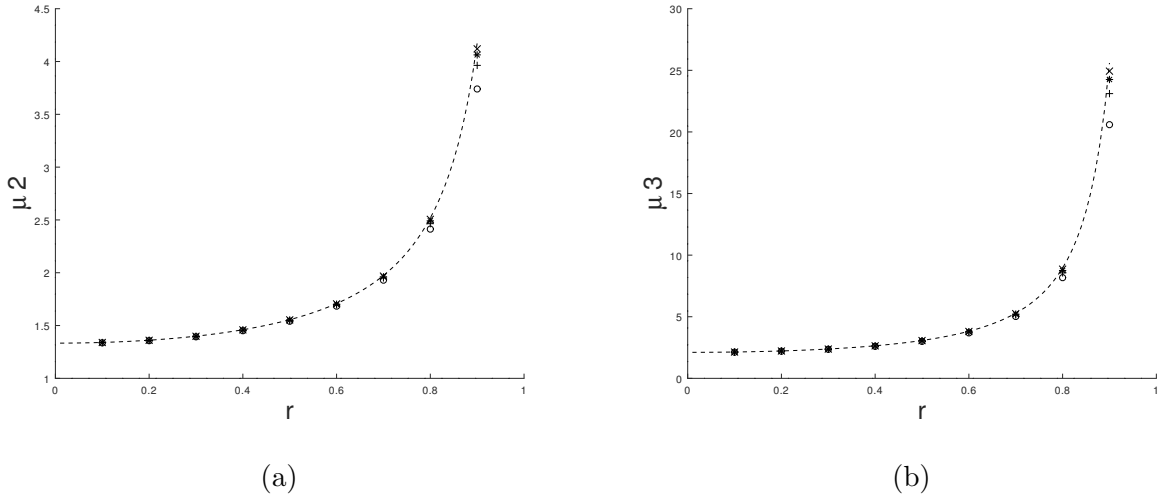


FIG. 2. The left figure shows the concentration of μ_2 and the right figure shows the concentration of μ_3 . The horizontal axis is r and the vertical axis is the second and third moments. Line styles: "o", "+", "*", "x", and the dotted lines indicate $N = 64, 128, 256, 512$ and theoretical moments, respectively. As the matrix size increases, the moments converge to the theoretical moments. Curves are averages of 1,000 replications and the moments are the averages.

ii. Convergence of the moments

Next, we confirm the convergence of the distributions for the fBm case. In Fig.4 we show μ_2 in $Q = 3, 6$ below $H_c = 3/4$, which is the transition point. Above $H_c = 3/4$, the second moment diverges. The horizontal axis is H and the vertical axis represents the second moment. As the matrix size increases, the moments converge to the theoretical moments. Appendix C presents the conclusions of the numerical simulations in detail.

V. PHASE TRANSITION OF THE DEFORMED MARCHENKO-PASTUR DISTRIBUTION

In this section, we study the phase transition in the case of power decay. We discuss the convergence of the scaled largest eigenvalue which is the order parameter of the phase transition in subsection A and apply finite scaling analysis to confirm the critical exponent in subsection B.

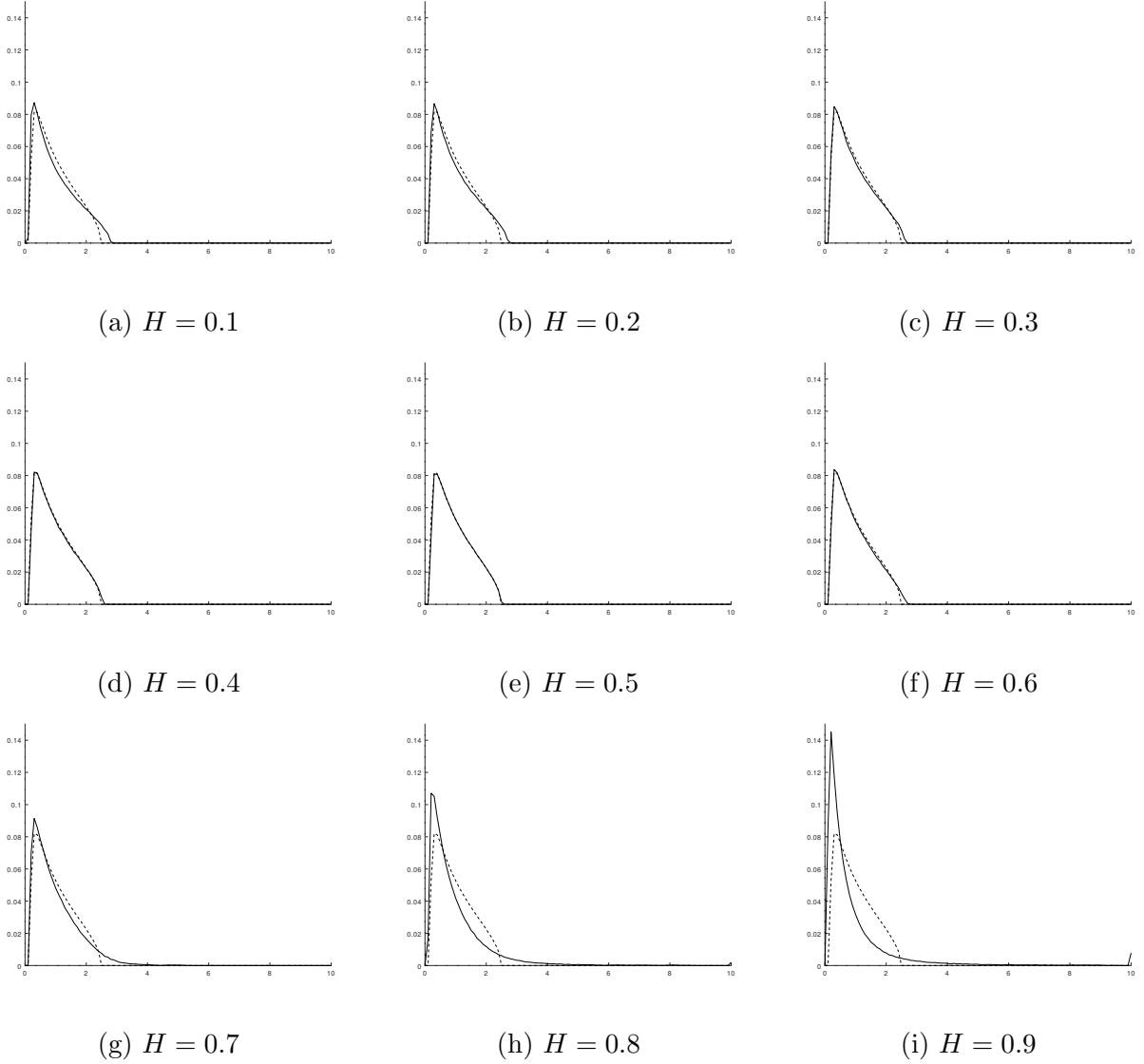


FIG. 3. Plots of the histogram of the deformed MPD for $Q = 3$ for fBm : (a) $H = 0.1$, (b) $H = 0.2$, (c) $H = 0.3$, (d) $H = 0.4$, (e) $H = 0.5$, (f) $H = 0.6$, (g) $H = 0.7$, (h) $H = 0.8$, (i) $H = 0.9$. The horizontal axis represents the eigenvalues and the vertical axis is the frequency. The real line is the distribution with the correlation and the dotted line is the MPD. We can confirm the fat tail distribution for large and small H .

A. The scaled largest eigenvalue and phase transition

In this subsection, we confirm the convergence of the scaled largest eigenvalue, $0 < x_1/N \leq 1$ in the case of fBm. In Fig.5 we show the scaled largest eigenvalues when $Q = 3$ and $Q = 6$. The horizontal axis is a log plot of matrix size N and the vertical axis is a

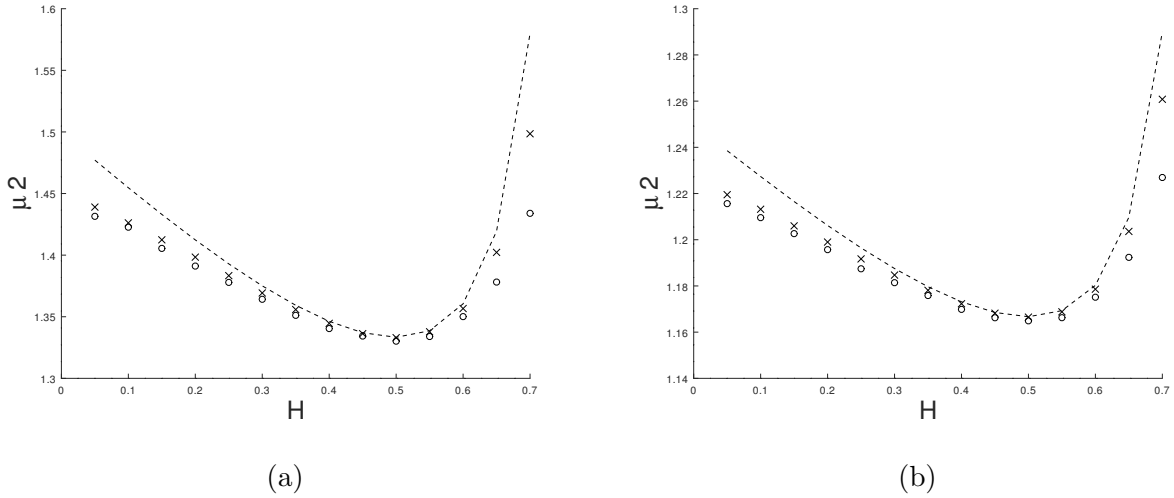


FIG. 4. The figure (a) shows μ_2 in $Q = 3$ and the figure (b) shows $Q = 6$ in the case of fBm. These are the comparisons between the theoretical moments and $N = 512, 64$ numerical simulations. The horizontal axis is H and the vertical axis is the second moment. "x", "o" indicate $N = 512, 64$ and the dotted lines show the theoretical moments.

log plot of the scaled largest eigenvalue x_1/N . When $H < H_c = 3/4$, the scaled largest eigenvalue is on a straight line and converges to 0, because the largest eigenvalue is finite. When $H \geq H_c = 3/4$, the scaled largest eigenvalue is not on a straight line. The dominance of the largest eigenvalue changes at H_c and increases above H_c . Therefore, the scaled largest eigenvalue is the order parameter of the phase transition.

B. Finite size scaling

In this subsection, we consider finite size scaling. We introduce the scaling function to the scaled largest eigenvalue, x_1/N , which we discussed in the previous subsection,

$$\frac{x_1}{N} = N^{\gamma/\nu} f(N^{1/\nu} t), \quad (22)$$

where $t = (H - H_c)/H_c$ and $f(x)$ is a scaling function. It is the hypothesis that the data of several N are on the curve, Eq.(22). We assume that the scaling function is $f(x) \sim 0$ in the limit $x \rightarrow -\infty$ and $f(x) \sim O(x)$ in the limit $x \rightarrow \infty$. In these hypotheses, we can obtain the following relation,

$$m \equiv \frac{x_1}{N} \propto t = (H - H_c)/H_c \quad H - H_c \gg N^{-1/\nu}$$

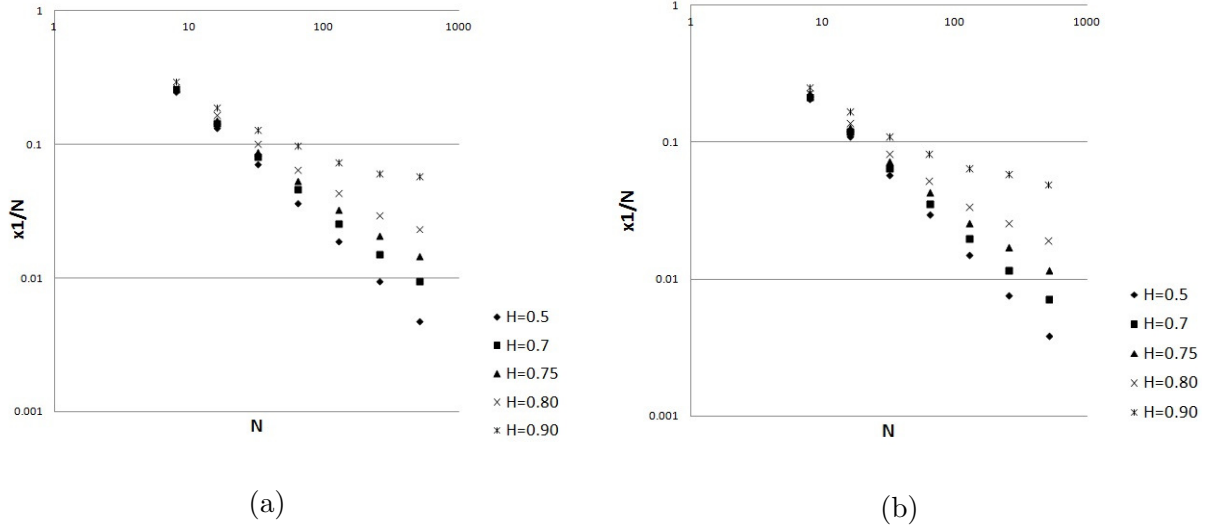


FIG. 5. Figures (a) and (b) show the scaled largest eigenvalue, x_1/N , when $Q = 3$ and $Q = 6$ for fBm. The horizontal axis is a log of the matrix size N , and the vertical axis is a log of the scaled largest eigenvalue x_1/N . We plot the cases $H = 0.5, 0.7, 0.75, 0.8, 0.9$. When $H < H_c = 3/4$, the scaled largest eigenvalue is on a straight line and converges to 0. When $H \geq H_c = 3/4$, the scaled largest eigenvalue is not on a straight line.

$$\propto 0. \quad H_c - H \gg N^{-1/\nu} \quad (23)$$

We confirmed convergence to 0 in the case, $H < H_C$ in the previous subsection.

We confirm this scaling hypothesis in Fig 6, where we set $\gamma = -1$ and $\nu = 4/3$. We estimate these parameters by setting that the data of several N are on the curve. The slope of the asymptotic line is 1 in large t , and it is consistent with Eq.(22) and Eq.(23).

Hence, we can estimate the critical exponent,

$$m \propto t^\beta \quad \text{at} \quad H \sim H_c \quad (24)$$

where $\beta = 1$ and

$$\xi_\infty \propto t^{-\nu} = t^{-4/3} \quad \text{at} \quad H \sim H_c, \quad (25)$$

where ξ_∞ is the correlation length.

VI. CONCLUDING REMARKS

We considered the time series with the correlation and its Wishart matrix. When the variables are independent, the eigenvalue distribution of the Wishart matrix converges to

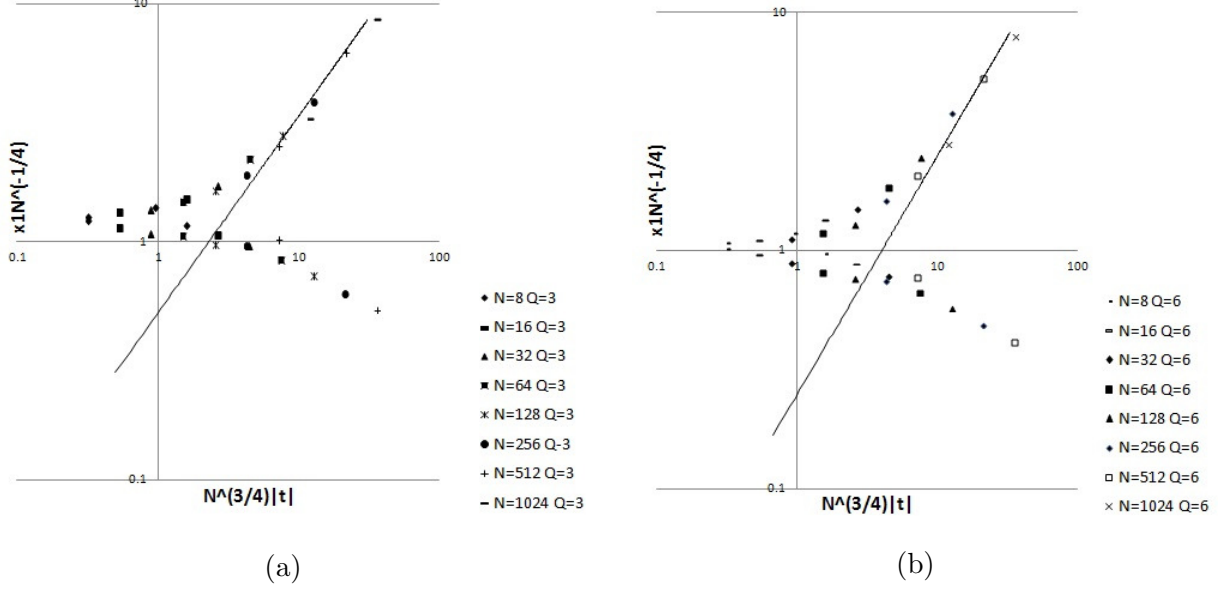


FIG. 6. Figures (a) and (b) show the finite size scaling plot when $Q = 3$ and $Q = 6$ in the case of power decay. The horizontal axis is a log of $N^{3/4}|t| = N^{3/4}|H - H_c|/H_c$, RHS of Eq.(22) and the vertical axis is a log of $x_1/N^{1/4}$, LHS of Eq.(22). Here we use $H_c = 3/4$. We can confirm that $N = 8, 16, 32, 64, 128, 256, 512, 1024$ are on a curve near the critical point and the asymptotic line is x which corresponds to the scaling function. The solid line is the asymptotic line t and the trend is 1 which is consistent with Eq.(23).

the Marchenko-Pastur distribution (MPD). When there is a correlation, the eigenvalue distribution converges to the deformed MPD. The deformed MPD has a long tail and a high peak for large temporal correlations. We calculated some moments of the distribution for the exponential and power decay cases and discussed the convergence of this distribution. We have shown that the mean of the distribution does not depend on the correlation and that the second moment increases as the temporal correlation increases. In particular when the temporal correlation is power decay, we can confirm a phenomenon such as phase transition from the finite second moment to the infinite second moment. In other words, it is the transition between the finite largest eigenvalue and the infinite largest eigenvalue. If $\gamma > 1/2$ which is the power index, the second moment of the distribution and the largest eigenvalue are finite. On the other hand, when $\gamma \leq 1/2$, the second moment and the largest eigenvalue are infinite. The largest eigenvalues, the explicit formula of the deformed MPD and the closed form of the higher moments, especially for the power decay case, are future

problems.

The other future problem is the study of phase transition for the power decay case. We discussed the convergence of the scaled largest eigenvalue which is the order parameter of the phase transition and applied finite scaling analysis and estimate the critical exponent. The theoretical confirmations are the future problems.

APPENDIX A THE MARCHENKO-PASTUR DISTRIBUTION AND ITS MOMENTS

In this Appendix, we review the moments of the Marchenko-Pastur distribution (MPD). The MPD is

$$P(\lambda) = \frac{Q}{2\pi\lambda} \sqrt{(\lambda_+ - \lambda)(\lambda - \lambda_-)},$$

where

$$\lambda_{\pm} = 1 + \frac{1}{Q} \pm 2\sqrt{\frac{1}{Q}},$$

and

$$Q = \frac{L}{N},$$

in the limit $N, L \rightarrow \infty$ with constant Q .

We can obtain the moment of the MPD

$$\begin{aligned} \mu_k &= E(\lambda^k) = \int_{\lambda_-}^{\lambda_+} \lambda^k P(\lambda) d\lambda \\ &= \frac{2}{\pi} \int_{-1}^1 [2\sqrt{\frac{1}{Q}}x + (1 + \frac{1}{Q})]^{k-1} \sqrt{1-x^2} dx, \end{aligned} \quad (26)$$

where

$$x = \frac{\lambda - (1 + \frac{1}{Q})}{2\sqrt{\frac{1}{Q}}}.$$

Here we divided the cases when $k = 2m + 1$ and $k = 2m + 2, m = 1, 2, \dots$.

In the case $k = 2m + 1$, we expand the first term by x and the odd powers of x become 0,

$$\begin{aligned} \mu_k &= \sum_{i=0}^m \binom{2m}{2i} C_i (1 + \frac{1}{Q})^{2m-2i} \frac{1}{Q^i} \\ &= \sum_{j=1}^k \sum_{i=0}^m \binom{2m}{2i} \binom{2m-2i}{j-1-i} C_i \frac{1}{Q^{j-1}} \end{aligned}$$

$$= \sum_{j=1}^k \frac{1}{k} \binom{k}{j} \binom{k}{j-1} \frac{1}{Q^{j-1}} \quad (27)$$

$$= \sum_{j=1}^k N(k, j) \frac{1}{Q^{j-1}} = \mathcal{N}_k\left(\frac{1}{Q}\right) \quad (28)$$

$N(k, j)$ is the Narayana number and $\mathcal{N}_k(x)$ is the Narayana polynomial. Then, the momentum of the MPD is the Narayana polynomial.

In the first first equal we use the relation

$$\int_{-1}^1 x^{2i} \sqrt{1-x^2} dx = \frac{\pi}{2^{2i+1}} C_i,$$

and C_i is the i the Catalan number

$$C_i = \frac{1}{i+1} \binom{2i}{i}. \quad (29)$$

In the second equal we use $j = i + l + 1$ instead of l . In the third equal we use the following identity,

$$\frac{1}{k} \binom{k}{j} \binom{k}{j-1} = \sum_{i=0}^{\lfloor (k-1)/2 \rfloor} \binom{k-1}{2i} \binom{k-2i-1}{j-1-i} C_i. \quad (30)$$

When $k = 2m + 2$ we can obtain in the same way

$$\begin{aligned} \mu_k &= \sum_{i=0}^m \binom{2m+1}{2i} C_i \left(1 + \frac{1}{Q}\right)^{2m+1-2i} \frac{1}{Q^i} \\ &= \sum_{j=1}^k N(n, j) \frac{1}{Q^{j-1}} = \mathcal{N}_k\left(\frac{1}{Q}\right). \end{aligned} \quad (31)$$

In summary we can obtain the moment μ_k for the MPD as Narayana polynomial [33],

$$\begin{aligned} \mu_1 &= 1 \\ \mu_2 &= 1 + \frac{1}{Q} \\ \mu_3 &= 1 + \frac{3}{Q} + \frac{1}{Q^2} \\ \mu_4 &= 1 + \frac{6}{Q} + \frac{6}{Q^2} + \frac{1}{Q^3} \\ \mu_5 &= 1 + \frac{10}{Q} + \frac{20}{Q^2} + \frac{10}{Q^3} + \frac{1}{Q^4} \\ \mu_6 &= 1 + \frac{15}{Q} + \frac{50}{Q^2} + \frac{50}{Q^3} + \frac{15}{Q^4} + \frac{1}{Q^5}. \\ \dots & \end{aligned} \quad (32)$$

APPENDIX B FRACTIONAL BROWNIAN MOTION

In this Appendix, we review the fractional Brownian motion (fBm). $H \in (0, 1)$ is the parameter of the fBm. When the Gauss process $B^H = \{B_t^H\}_{t \geq 1}$ with $E(B^H) = 0$ satisfies following condition, the process is the fBm,

$$\text{Cov}(B_s^H, B_t^H) = \frac{1}{2}(|t|^{2H} + |s|^{2H} - |t - s|^{2H}), \quad (33)$$

in any t and s . H is the Hurst index. In the case $H = 1/2$, the process is Brownian motion. In the case $H \neq 1/2$, the process has a power decay temporal correlation with $\gamma \sim 2 - 2H$ in $t \gg 1$. Here γ is the power index. Hence, when $H > 1/2$, the process has long memory and $H < 1/2$ the process has short memory.

APPENDIX C CONVERGENCE TO THE THEORETICAL VALUES OF THE DEFORMED MPD

In this Appendix we compare the theory and numerical simulations. We show the cases $Q = 3$ and $Q = 6$ of exponential decay temporal correlation in Tables.III and IV, respectively. In Tables.V and VI we show the cases of the fBm in $Q = 3, 6$. At $H = 3/4$ μ_2 becomes infinite.

APPENDIX D PROPERTIES OF THE FINANCIAL TIME SERIES DATA

Table VII shows the properties of the data in section I [34]. We chose six characteristic time series from [22] and showed the properties of these time series. Three of them are FX, two are commodities, and one is a stock index. As mentioned in section I, we chose three FX time series that have large temporal correlations. Compared to stock and bond prices, FX has a strong temporal correlation, meaning that they swing in one direction and tend to stay that way. The temporal correlation is sometimes the trend created by the central banks and governments.

TABLE III. Comparison of the moments between the simulations and theory for $Q = 3$

r	0	0.1	0.2	0.3	0.4	0.5	0.6	0.7	0.8	0.9
$N = 512, \mu_2$	1.3329	1.3396	1.3605	1.3984	1.4591	1.5537	1.7053	1.9681	2.5047	4.1215
$N = 64, \mu_2$	1.3295	1.3364	1.3565	1.3934	1.4508	1.5405	1.6836	1.9297	2.4130	3.7446
Theory μ_2	1.3333	1.3401	1.3611	1.3993	1.4603	1.5556	1.7083	1.9739	2.5185	4.1754
$N = 512, \mu_3$	2.1092	2.1362	2.221	2.3775	2.6378	3.0651	3.8058	5.2536	8.8539	24.9533
$N = 64, \mu_3$	2.0950	2.1228	2.2034	2.3549	2.5986	2.9993	3.6891	5.0216	8.1719	20.5884
Theory μ_3	2.11111	2.13812	2.22338	2.38137	2.64324	3.07407	3.82205	5.28861	8.95885	25.59588
$N = 512, \mu_4$	3.698	3.7792	4.0378	4.5286	5.3836	6.8831	9.746	16.1855	36.184	173.524
$N = 64, \mu_4$	3.6555	3.7394	3.9837	4.4554	5.2481	6.6385	9.2643	15.0777	32.0347	130.7156
Theory μ_4	3.70370	3.80732	4.13587	4.75033	5.78594	7.53909	10.73691	17.59557	38.10822	180.77500

APPENDIX E PERTURBATION OF THE WISHART MATRICES

In this Appendix, we consider the moments of perturbation of the Wishart matrices. We consider the following matrix,

$$(A_\mu, A_{\mu+L}, \dots, A_{(N-1)\mu+L}) = \xi^\mu \mathbf{B} / \sqrt{b^2 + 1} + \epsilon^\mu / \sqrt{b^2 + 1}, \quad (34)$$

where $\mu = 1, 2, \dots, L$ and \mathbf{B} , and ϵ are the size N vectors. A_i is the element of Eq.(4). The elements of ϵ and ξ^μ are i.i.d. All elements of \mathbf{B} are b . The first term corresponds to the perturbation from the random matrix. The second moment of the eigenvalue is

$$\begin{aligned} \mu_2 &= \frac{1}{L^2 N} \sum_{\nu_1=1}^L \sum_{\nu_2=1}^L \sum_{m_1=1}^N \sum_{m_2=1}^N \langle A_{m_1\nu_1}^T A_{\nu_1 m_2} A_{m_2\nu_2}^T A_{\nu_2 m_1} \rangle \\ &= 1 + \frac{1}{Q} + \left(\frac{b^2}{b^2 + 1}\right)^2 \frac{N(N-1)L^2}{N^3 L^2} = 1 + \frac{1}{Q}, \end{aligned} \quad (35)$$

in the limit of $N, L \rightarrow \infty$ with $L/N = Q$. The second moment is the same as MPD. In the same way we can calculate the higher moments which are the same as MPD. In this model the correlation is smaller than that in our model. These conclusions are consistent with the following transition of the largest eigenvalue in this model [30]. The transition point is

TABLE IV. Comparison of the moments between the simulations and theory for $Q = 6$

r	0	0.1	0.2	0.3	0.4	0.5	0.6	0.7	0.8	0.9
$N = 512, \mu_2$	1.1671	1.1698	1.1802	1.1992	1.2295	1.2771	1.3532	1.4853	1.7554	2.5731
$N = 64, \mu_2$	1.1647	1.1675	1.1782	1.19660	1.2260	1.2718	1.3455	1.4716	1.7247	2.4649
Theory μ_2	1.16667	1.17003	1.18056	1.19963	1.23016	1.27778	1.35417	1.48693	1.75926	2.58772
$N = 512, \mu_3$	1.5294	1.5386	1.5753	1.6432	1.7536	1.9322	2.2326	2.7954	4.1076	9.418
$N = 64, \mu_3$	1.5209	1.5308	1.5681	1.6337	1.7400	1.9112	2.1998	2.7308	3.9402	8.5995
Theory μ_3	1.52778	1.53958	1.57668	1.64479	1.75605	1.93519	2.23676	2.80254	4.12860	9.53055
$N = 512, \mu_4$	2.1756	2.1986	2.2924	2.4685	2.7634	3.2614	4.1568	6.0069	11.0852	39.8625
$N = 64, \mu_4$	2.1540	2.7193	2.2740	2.4436	2.7257	3.2013	4.0535	5.7781	10.3701	34.7996
Theory μ_4	2.17129	2.21626	2.35784	2.61857	3.04684	3.74331	4.93717	7.25797	13.15499	43.86338

TABLE V. Comparison of the moments between the simulations and theory for fBm in $Q = 3$

H	0.1	0.2	0.3	0.4	0.5	0.6	0.7	0.8	0.9
$N = 512, \mu_2$	1.4261	1.3982	1.369	1.3448	1.3331	1.3568	1.4991	2.1279	4.7319
$N = 64, \mu_2$	1.4159	1.3894	1.3648	1.3407	1.3289	1.3485	1.4338	1.6687	2.2148
Theory	1.454	1.412	1.375	1.346	1.333	1.360	1.579	N.A.	N.A.

$Qb_c^4 = 1$. Here we set the eigenvector of the largest eigenvalue as \mathbf{e}_1 . The order parameter of the phase transition is $|\hat{m}| = \mathbf{e}_1^T \cdot \mathbf{B}/N$ which is the direction cosine. The critical exponent is,

$$|\hat{m}| \propto t^\beta = ((b^2 - b_c^2)/b_c^2)^\beta \quad \text{at} \quad b^2 \sim b_c^2 \quad (36)$$

where $\beta = 1/2$ and

$$\xi_\infty \propto t^{-\nu} = t^{-3} \quad \text{at} \quad b^2 \sim b_c^2, \quad (37)$$

where ξ_∞ is the correlation length [30].

TABLE VI. Comparison of the moments between the simulations and theory for fBm in $Q = 6$

H	0.1	0.2	0.3	0.4	0.5	0.6	0.7	0.8	0.9
$N = 512, \mu_2$	1.2130	1.1989	1.1846	1.1723	1.1663	1.1787	1.2603	1.7062	3.9633
$N = 64, \mu_2$	1.2105	1.1964	1.1827	1.1705	1.1647	1.1743	1.2274	1.3901	1.8394
Theory	1.227	1.206	1.188	1.173	1.1667	1.180	1.290	N.A.	N.A.

TABLE VII. Data spec of Table VII where USD is US Dollar. CAD is Canadian Dollar, EUR is Euro, GBP is Britain Pound, Soy is the commodity price of beans, VIX is the volatility index, and NKY 225 is the index of Japanese stock market.

no.	data name	data category	data period	data interval	data length
1	USD/CAD	FX (natural resource)	2021/5/19 20:22-2021/7/15 19:57	minutely	60,000
2	EUR/CHF	FX (cross pair)	2021/5/18 13:20-2021/7/15 20:00	minutely	60,000
3	EUR/GBP	FX (cross pair)	2021/5/19 1:06-2021/7/15 20:00	minutely	60,000
4	SOY	commodity	2021/4/19 9:01-2021/7/15 19:57	minutely	38,483
5	VIX	commodity	2021/4/15 20:11-2021/7/15 19:56	minutely	48,106
6	NKY225	stock index	1965/1/5-2021/7/15	daily	14,886

APPENDIX F CORRELATED TIME SERIES

In this Appendix we review how to create the correlated time series. We create \mathbf{A}_μ from the non-correlated normal distribution, $\mathbf{A}_{0\mu}$ where

$$\mathbf{A}_0 = (\mathbf{A}_{01}, \mathbf{A}_{01+L}, \dots, \mathbf{A}_{01+(N-1)L}), \quad (38)$$

and $\mathbf{A}_{0\mu} = (A_{0\mu}, \dots, A_{0\mu+L-1})^T$, $\mu = 1, 1+L, \dots, 1+(N-1)L$, the size L vector.

The distribution \mathbf{A}_μ is the correlated normal distribution,

$$f(\mathbf{A}_\mu) = \frac{1}{(2\pi)^{\frac{L}{2}} |D_{L-1}|} \exp[-\frac{1}{2} \mathbf{A}_\mu^T D_{L-1}^{-1} \mathbf{A}_\mu]. \quad (39)$$

Here we set

$$\mathbf{A}_\mu = \sqrt{\Pi} \mathbf{A}_{0\mu}. \quad (40)$$

The distribution of $\mathbf{A}_{0\mu}$, $g(\mathbf{A}_{0\mu})$ is

$$g(\mathbf{A}_{0\mu}) = f(\mathbf{A}_\mu) \left| \frac{\mathbf{A}_\mu}{\mathbf{A}_{0\mu}} \right| = \frac{|\sqrt{\Pi}|}{(2\pi)^{\frac{L}{2}} |D_{L-1}|} \exp\left[-\frac{1}{2} \mathbf{A}_{0\mu}^T \sqrt{\Pi}^T D_{L-1}^{-1} \sqrt{\Pi} \mathbf{A}_{0\mu}\right]. \quad (41)$$

When $\sqrt{\Pi}^T D_{L-1}^{-1} \sqrt{\Pi} = \mathbf{1}$, the distribution, $g(\mathbf{A}_{0\mu})$ is

$$g(\mathbf{A}_{0\mu}) = \frac{1}{(2\pi)^{\frac{L}{2}} |D_{L-1}|} \exp\left[-\frac{1}{2} \mathbf{A}_{0\mu}^T \mathbf{A}_{0\mu}\right], \quad (42)$$

and Eq.(6). This is the non-correlated normal distribution.

* hisakadom@yahoo.co.jp

† tkaneko@icu.ac.jp

- [1] M.L. Mehta, *Random matrices* (3rd edition) , Elsevier (2004).
- [2] G. Akemann, J. Baik, and P.Di Francesco (Editors), *The oxford Handbook of Random Matrix Theory*, Oxford Univ.Press (2011)
- [3] D.C. Hoyle and M. Rattay, *Phys. Rev. E.* **69(2)** 026124 (2004)
- [4] T Hastie, A. Montanari, S. Rosset, and R.J. Tibshirani, *Annals of Stat* **50(2)** 949
- [5] L. Lalux, P. Cizeau, J.-P. Bouchaud, and M. Potters *Phys Rev. Lett.* **83** 1467 (1999)
- [6] M. Potters and J.-P. Bouchaud *Theory of Financial Risk and Derivative Pricing: From Statistical Physics to Risk Management* Cambridge university press (2003)
- [7] M.Potters and J.-P. Bouchaud *A first course in random matrix theory* Cambridge university press (2021)
- [8] A. Chakraborty, T Hatsuda, and Y Ikeda, *Sci Rep* **12(1)** 4718(2023)
- [9] A. Chakraborty, T Hatsuda, and Y Ikeda, *Dynamic relationship between XRP price and correlation tensor spectra of the transaction network.* **arXiv:2309.05935** (2023)
- [10] J. Wishart, *Biomet* **20A** 32 (1928)
- [11] R.A.Fisher. *Biomet* **10(4)** (1915)
- [12] V.A. Marčenko and L.A. Pastur *Math of USSR-Sbornik* **1(4)** 457 (1967)
- [13] M. Chiani, M.Z. Win, and A.Zenella, *IEEE Trans. Inf. Theory* **49(10)** 2363 (2003)
- [14] S.H.Simon, A.L. Moustakas, and L. Marinelli, *IEEE Trans. Inf. Theory* **52(12)** 5336 (2006)
- [15] V.V. Veeravalli, Y. Liang, and A.M. Sayeed, *IEEE Trans. Inf. Theory* **51(6)** 2058 (2005)
- [16] Y.Karasawa, *IEEE Trans. Vehicul. Technol* **69(5)** 5330 (2020)

- [17] I. Florescu, M. C. Mariani, H. E. Stanley, and F. G. Viens (Eds.) *Handbook of High-Frequency Trading and Modeling in Finance* John Wiley& Sons (2016)
- [18] F. Biagini, Y. Hu, B. Øksendal, and T Zhang *Stochastic calculus for fractional Brownian motion and applications* Springer Science and Business Media (2008)
- [19] S. Rostek, R Schöbel *Econ Modeling* **30** 30 (2013)
- [20] B.B. Mandelbrot and J.W. Van Ness, *SIAM rev* **10(4)** 422 (1968)
- [21] M T Greene and B D Fielitz *J. Fin Econ* **4(3)** 339 (1977)
- [22] T. Kaneko, M Hisakado, *Random Matrix Theory (RMT) Application on Financial Data* In: Aruka, Y. (eds) *Digital Designs for Money, Markets, and Social Dilemmas. Evolutionary Economics and Social Complexity Science* **28** Springer 347 (2022)
- [23] T Jamali1 and G. R. Jafari1, *Europhys Lett* **111** 10001 (2015)
- [24] R. Kühn1 and P. Sollich, *Europhys Lett* **99** 20008 (2012)
- [25] J.P. Kermoal, L. Schumacher, K.I. Pedersen and P. Mogensen *IEEE J. Selec. Areas. Commun* **20(6)** 1211 (2002)
- [26] J. Kwapieńa, and S Drożdż *Phy. Rep* **515** 115 (2012)
- [27] K.E. Bassler, P.J. Forrester, N.E. Frankel, *J. Math. Phys.* **50** 033302 (2009)
- [28] J. Baik, G. Ben arous, S. Péché, *Ann. Prob.* *33* 1643 (2005)
- [29] F Benaych-Georges and R R Nadakuditi, *Adv in Math* 494 (2011)
- [30] D.C. Hoyle, M. Rattay, *Phy Rev. E.* **69(2)** 026124 (2004)
- [31] M. Hisakado and S. Mori, *Physica A*, **544** 123480 (2020)
- [32] M Hisakado, S Mori, *Physica A* **563**, 125435 (2021).
- [33] X Yang, R Itoi, M Tanaka-Yamawaki, *Prog Theo Phy Supp* **194** 73 (2012)
- [34] The financial time series data is form Bloomberg.